

Evaluation of epifluorescence methods for quantifying bioaerosols in fine and coarse particulate air pollution



L.-W. Antony Chen^{a,b,*}, Mi Zhang^b, Ting Liu^c, Karey Fortier^a, Judith C. Chow^{b,d},
Fernanda Alonzo^a, Rachel Kolberg^{a,1}, Junji Cao^d, Ge Lin^a, Tanviben Y. Patel^a, Patricia Cruz^a,
Mark P. Buttner^a, John G. Watson^{b,d}

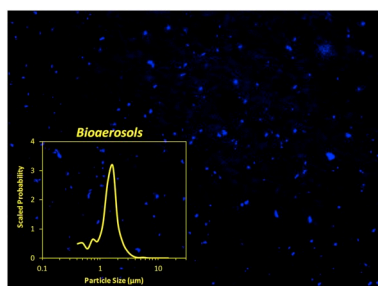
^a Department of Environmental and Occupational Health, School of Public Health, University of Nevada Las Vegas, Las Vegas, NV, 89154, USA

^b Division of Atmospheric Sciences, Desert Research Institute, Reno, NV, 89512, USA

^c School of Environmental Science & Engineering, Hubei Polytechnic University, Hubei Key Laboratory of Mine Environmental Pollution Control and Remediation, Huangshi, 435003, China

^d Key Laboratory of Aerosol Chemistry & Physics (KLACP), Institute of Earth Environment, Chinese Academy of Sciences, Xi'an, 710061, China

GRAPHICAL ABSTRACT



ARTICLE INFO

Keywords:

Primary biological aerosol particles
Automated particle counting
Aerosol size distribution
DNA stain
PM₁₀
PM_{coarse}

ABSTRACT

Despite being recognized as an important part of particulate matter (PM) air pollution and health risk, bioaerosols have not been quantified as extensively as other PM components for establishing PM standards and management strategies. The challenge lies partly in the lack of practical measurement methods. This study evaluated a filter-based, direct-staining fluorescence microscopy (DS-FM) method that may be adapted to routine air quality monitoring for bioaerosol concentration and size distribution. Through testing with bioaerosol standards made of bacterial cells and fungal spores, the method is shown to have precision, accuracy, detection limit, and dynamic range suitable for most ambient environments. DS-FM was demonstrated with PM samples from an arid urban location in Las Vegas, Nevada during the spring allergy season. Detectable bioaerosols ranged from 0.37 to 16 μm in geometric diameter and averaged $0.27 \pm 0.23 \text{ cm}^{-3}$ in number concentration with about 2/3 and 1/3 in the fine ($\leq 2.5 \mu\text{m}$) and coarse ($> 2.5 \mu\text{m}$) mode, respectively. The bioaerosol mass, estimated from the size distribution and an assumed density, was mainly in the coarse mode and accounted for $17 \pm 11\%$ of PM₁₀, $20 \pm 13\%$ of PM_{10-2.5}, and $4 \pm 3\%$ of PM_{2.5} mass. Rain and high wind speeds appeared to elevate bioaerosol levels. Other advantages of DS-FM include low sample consumption and short turnaround times; a large amount of data can be generated by incorporating the measurement into current long-term air quality

* Corresponding author. Department of Environmental and Occupational Health, School of Public Health, University of Nevada Las Vegas, Las Vegas, NV, 89154, USA.

E-mail address: antony.chen@unlv.edu (L.-W.A. Chen).

¹ Currently with Clark County Department of Air Quality, Las Vegas, NV 89118.

<https://doi.org/10.1016/j.atmosenv.2019.05.051>

Received 27 December 2018; Received in revised form 14 May 2019; Accepted 18 May 2019

Available online 24 May 2019

1352-2310/ © 2019 Elsevier Ltd. All rights reserved.

networks. Suggestions for using the data to inform bioaerosol origins, contributions, and public health impacts are discussed.

1. Introduction

Primary biological aerosol particles (PBAP), commonly referred to as bioaerosols, consist of airborne bacteria, viruses, fungi, pollen, microalgae, protozoa, plant detritus, insect fragments, animal fur, and cell fragments resulting from natural and anthropogenic processes. The diverse sources of bioaerosols lead to a complex size distribution (10 nm–100 μm) and heterogeneous spatiotemporal variability. Bioaerosols have been associated with adverse human health effects, particularly in occupational and indoor environments, and some are irritants in the upper respiratory tract and triggers for allergies and asthma (Douwes et al., 2003; Mauderly and Chow, 2008; Walser et al., 2015). Outdoor bioaerosols also affect cloud formation and climate (Deguillaume et al., 2008). Bioaerosols can contribute to airborne particulate matter (PM), especially coarse PM (termed $\text{PM}_{10-2.5}$) in the size range of 2.5–10 μm (Després et al., 2012; Fröhlich-Nowoisky et al., 2016). However, they have not been included as part of long-term air quality monitoring and are seldom evaluated in receptor- and source-oriented source apportionment models. An exposure limit for bioaerosols has not been established (Walser et al., 2015). The extent to which bioaerosols influence non-compliance with National Ambient Air Quality Standards (NAAQS) for $\text{PM}_{2.5}$ and PM_{10} (particulate matter mass with aerodynamic diameters < 2.5 and < 10 μm , respectively) is also unknown (U.S. EPA, 2006).

PM monitoring networks sample particles on various filter substrates for offline analysis of mass and, at times, bulk chemical composition at hundreds of locations with 24-h resolution (Chow et al., 1995; Hand et al., 2012). Quantifying bioaerosols (or their surrogates) in these networks can address the aforementioned knowledge gaps. A desirable bioaerosol measurement technique would be compatible with the conventional PM sampling systems while requiring minimal sample preparation, a relatively short turnaround time, and low cost. Bioaerosol size distributions are desirable to estimate transport distances, residence times, and penetration into the human respiratory tract (Fröhlich-Nowoisky et al., 2016). Although real-time fluorescence techniques such as the Ultraviolet-Aerodynamic Particle Sizer (UV-APS), the Waveband Integrated Bioaerosol Sensor (WIBS), and more recently the Spectral Intensity Bioaerosol Sensor (SIBS) show potential for resolving bioaerosol size-number concentration, sub-hourly temporal variation, and some classification (Healy et al., 2014; Nasir et al., 2019), the high cost may prevent them from being extensively deployed for the networks.

Polyalcohol compounds, such as arabinol and mannitol, have been measured on filter samples to indicate fungal spores, while endotoxin and (1 \rightarrow 3)- β -D-glucan serve as surrogates for the bacteria- and fungi-related toxicity, respectively (Boeson et al., 2004; Chow et al., 2015; Zhang et al., 2015; Gosselin et al., 2016). However, these molecular markers only represent a subset of bioaerosols. More detailed speciation may be achieved by polymerase chain reaction (PCR) with specific deoxyribonucleic acid (DNA) primers (Fröhlich-Nowoisky et al., 2009). Universal primers for total bacteria or fungi abundances have also been developed, but improvements in their sensitivity, precision, and throughput are warranted (Peccia and Hernandez, 2006; Blais-Lecours et al., 2015). Both the molecular marker and PCR methods offer little information on bioaerosol size and number concentration.

Microscopic methods, including epifluorescence microscopy, detect individual particles. Based on particle size and morphology, it is possible to quantify bio- and other aerosol abundances (Chow et al., 2015; Wagner and Macher, 2012; Tai et al., 2017). Specific DNA or protein stains are available to mark bioaerosols and distinguish between viable and nonviable fractions under a fluorescence microscope (Li and

Huang, 2006). The classical approach extracts particles from a filter into a liquid where the particles are stained, and subsequently re-deposited on another substrate for microscopic analysis (Wiedinmyer et al., 2009; Dong et al., 2016). This procedure is referred to as Extraction-Staining Fluorescence Microscopy (ES-FM). A more convenient alternative, known as Direct-Staining Fluorescence Microscopy (DS-FM), applies stain(s) directly onto the filter (Prussin et al., 2015; Perrino and Marcovecchio, 2016). DS-FM can potentially meet the requirements for routine bioaerosol monitoring. However, the accuracy, precision, and dynamic range of either ES-FM or DS-FM have not been evaluated for PM samples, nor has their potential of resolving bioaerosol size distribution from fluorescence images been assessed.

This paper documents a DS-FM method for quantifying bioaerosol number and mass concentrations, as well as size distribution, in $\text{PM}_{2.5}$ and PM_{10} samples. For the first time, the method is assessed for measurement accuracy and precision using laboratory generated bioaerosol standards. Further evaluations involve applying DS-FM to ambient PM samples collected in Las Vegas, Nevada during the peak allergy season and comparing the results with concurrent pollen grain/fungal spore counts, PM mass, and values reported in the literature by different techniques. The potential of implementing this measurement in air quality networks and using the data to investigate bioaerosol sources and impacts are also discussed.

2. Experiments

2.1. Bioaerosol standards and ambient samples

To characterize the DS and ES fluorescence methods, standard samples with known bioaerosol concentrations were prepared using reference bacteria (*Escherichia coli*, American Type Culture Collection [ATCC] 25922, Manassas, Virginia, USA) and fungal spores (*Aspergillus fumigatus*, ATCC 36607). The bacterial cells and fungal spores were initially suspended in deionized (DI) water at levels of $7.4 \times 10^8 \text{ ml}^{-1}$ and $4.0 \times 10^8 \text{ ml}^{-1}$, respectively, as determined by hemocytometer counting. After a series of dilutions, the cells and spores were deposited onto 13-mm-diameter black polycarbonate (BPC) filter discs (PCTE, 0.2- μm pore size, GVS North America, Sanford, ME, USA) by syringe filtration. BPC filters were selected due to their low fluorescence background and flat surface suitable for microscopic imaging. Five concentration levels of *E. coli* on the filters were prepared: 5.6×10^3 , 2.8×10^4 , 5.6×10^4 , 2.8×10^5 , and $5.6 \times 10^5 \text{ cm}^{-2}$. These loadings correspond to a range of 0.01–1 cm^{-3} ambient bioaerosols if the bioaerosols are sampled through a 47-mm-diameter filter at 5 L min^{-1} for 24 h (i.e., 7.2 m^3 air sampled through 13.85 cm^2 deposit area) with a MiniVol sampler (Airmetrics, Springfield, OR, USA). As for fungal spores, loadings of 1.5×10^4 , 3.0×10^4 , 7.5×10^4 , 1.5×10^5 , and $3.0 \times 10^5 \text{ cm}^{-2}$ were prepared on BPC filters, corresponding to 0.03–0.6 cm^{-3} ambient bioaerosol concentrations sampled by a MiniVol for 24 h. Blank samples were also prepared by pushing DI water through the filter to determine lower quantifiable limits (LQL) (Kolberg, 2017).

Ambient $\text{PM}_{2.5}$ and PM_{10} samples were acquired on the rooftop of a three-story building at the University of Nevada, Las Vegas (UNLV) campus (Supplemental Fig. S1) during spring (April 1 to May 31) 2017 using two pairs of MiniVol samplers equipped with 2.5 or 10 μm (aerodynamic diameter) size-selective inlets. This site has an urban-scale zone of representation and is > 300 m from busy roadways. Elevated pollen concentrations during spring are the most noticeable bioaerosols in the Las Vegas metro area (CCDAQ, 2014), which is one of the cities most affected by seasonal allergies in the western U.S. (AAFA,

2018).

Twenty-four-hour sampling took place each day from midnight to midnight. Air was drawn through 47-mm diameter BPC filters with a 42-mm diameter deposit area, from which up to six 13-mm diameter discs could be removed for analysis (Fig. S2). A Burkard spore trap (Burkard Manufacturing Company, Rickmansworth, UK) was collocated for pollen and fungal spore quantification based on microscopic identification and counting as part of the National Allergy Bureau (NAB) network (Portnoy et al., 2004). At a 24-h time resolution, common pollen (maple, ash, mulberry, olive, pine, sycamore, and elm) and spore (*Alternaria*, *Cladosporium*, Smuts/Myxomycetes, Undifferentiated Ascospores, and Undifferentiated Basidiospores) taxa of allergic concerns have been reported, in m^{-3} , to the NAB Pollen and Mold Report (Patel et al., 2018a, 2018b).

The Clark County Department of Air Quality (CCDAQ) monitors $\text{PM}_{2.5}$ and PM_{10} across the Las Vegas valley as part of the U.S. EPA compliance network with stations relative to the UNLV site shown in Fig. S1 (Supplementary Information). Spatially averaged PM concentrations determined the air quality index (AQI) and were compared with bioaerosol levels at UNLV to evaluate bioaerosol contributions to $\text{PM}_{2.5}$ and PM_{10} in Las Vegas. Weather data including wind speeds and wind directions were acquired from the McCarran International Airport, ~2 km southwest of the UNLV monitoring site. The PM and meteorological data are presented in Fig. S3.

2.2. Staining and microscopic imaging

For the DS method, $20 \mu\text{g ml}^{-1}$ of 4',6-diamidino-2-phenylindole (DAPI, Fisher Sci., Hampton, NH, USA) was placed on a clean microscope slide onto which the 13-mm diameter filter disc (from an equilibrated standard or ambient sample) was placed with the exposed side facing up. This approach allowed the stain to permeate through the filter and interact with the particle deposit while avoiding excess stain on the deposit side which could increase the fluorescence background (Griffin et al., 2001). DAPI marks both living and dead cells with blue fluorescence (Kepner and Pratt, 1994). Other stains such as acridine orange and bisbenzimidazole were tested, but they produced higher background fluorescence and therefore lower signal-to-noise ratios than DAPI. Stained samples were incubated for 20 min in the dark, and then a glass coverslip was placed over the stained filter with a water-soluble, anti-bleaching adhesive (Fluoromount-GTM, Southern Biotech, Birmingham, AL, USA). The samples were examined immediately and archived at $< 4^\circ\text{C}$ after epifluorescence examination.

Ambient samples were also subjected to ES, for which particles were extracted from the samples and stained in the colloid phase. One quarter of each 47-mm filter was transferred to a centrifuge tube containing 1 ml DI water and vortexed for 5 min. Ten μl of a $500 \mu\text{g ml}^{-1}$ DAPI stain was added to the extracted colloid of 0.25 ml producing $\sim 20 \mu\text{g ml}^{-1}$ DAPI concentration, and incubated for 20 min in the dark. The stained extract was drawn through a blank 13-mm diameter

BPC filter on which the solid particles remain; this filter was then mounted on a microscope slide prior to epifluorescence microscopy (Fig. S2). In principle, this ES procedure may be applied to different filter media, including the Teflon-membrane and quartz-fiber filters commonly used in PM compliance and speciation networks.

The DS or ES sample slides were analyzed with a fluorescence microscope (BX51, Olympus, Tokyo, Japan) with excitation and emission wavelengths centered at 350 nm and 460 nm, respectively, specific for DAPI bound to DNA. Fluorescence images were recorded by a charge coupled device (CCD) camera (DP70, Olympus, Tokyo, Japan). The microscope/camera system was optimized for contrast and remained the same for all samples. At least 30 images of random fields of view ($0.22 \times 0.166 \text{ mm}^2$) were captured for each sample at 400X microscope magnification to represent the entire 13-mm diameter deposit area. This imaging process required < 10 min per sample. A wide range of bioaerosol sizes and morphologies were observed in ambient samples. Loss of color (e.g., photobleaching) was not apparent during the first examination (~ 5 s each field of view), making it possible for repetitive analyses of the same samples.

Nonhomogeneous PM deposits increase uncertainties as each filter punch is intended to represent the entire deposit area. To evaluate measurement precision, triplicate analyses were performed for all DS-FM measurements by preparing three or more sets of standards and acquiring a minimum of three punches from each ambient sample. For ES-FM, only duplicate analyses were performed, because the technique requires a larger sample size and greater effort. In addition, punches from four ambient samples were spiked with *E. coli* in the same way as the standard samples to investigate interferences of non-biogenic PM with bioaerosol measurements.

2.3. Particle number, size, and mass calculations

Automated bioaerosol enumeration from fluorescence images was achieved using the ImageJ[®] software as demonstrated for Scanning Electron Microscopy (SEM) images by Tai et al. (2017). Images were gray-scaled and then converted to binary (black-and-white) pictures with the fluorescent particles in black and background in white (Fig. 1). The threshold required to distinguish between particles and background was determined by the “Triangle” algorithm (Zack et al., 1977; Seo et al., 2014). To suppress false positives, particles occupying fewer than five pixels were excluded. ImageJ[®] then quantified the number of fluorescent particles in the image and the projected area (A_p) of each particle, yielding equivalent projected area diameters ($D_{eq,A}$):

$$D_{eq,A} = 2 \left(\frac{A_p}{\pi} \right)^{1/2} \quad (1)$$

The cut-off $D_{eq,A}$ was $\sim 0.37 \mu\text{m}$, which should be sufficient to detect most bacteria, fungal spores, and other major mass contributing bioaerosols. Using 1000X instead of 400X magnification only lowered

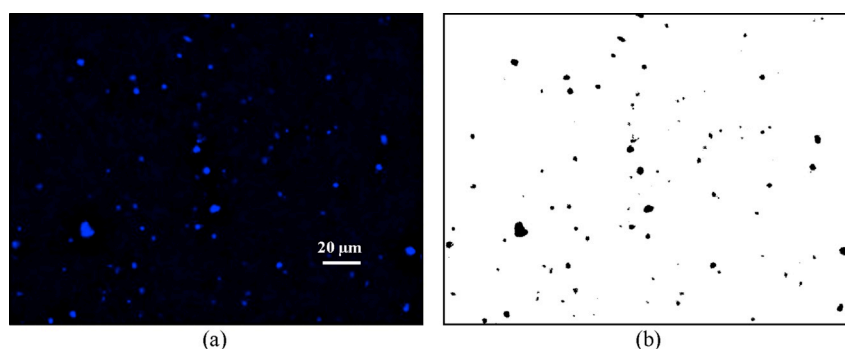


Fig. 1. An example of: (a) original and (b) processed fluorescence image (1360×1024 pixels). This is a PM_{10} sample acquired on 5/16/2017. Particles occupying fewer than five pixels were excluded from bioaerosol counting, leading to a size detection limit of $0.37 \mu\text{m}$.

the cut-off $D_{eq,A}$ slightly (i.e., to $\sim 0.28 \mu\text{m}$). However, the higher magnification required an oil-immersion lens and doubled the imaging time.

For each individual sample slide, bioaerosol number concentration was determined from the mean particle counts (excluding outliers) over all fluorescence images taken for the sample. Outliers were defined as either: 1) counts more than the median count plus 1.5 times the interquartile range, or 2) counts less than the median count minus 1.5 times the interquartile range (Navidi, 2008), which could result from physical contamination, particle loss, and/or image processing difficulties. The standard error of the mean provides an estimate of uncertainty in number concentrations. These uncertainties decrease as the number of images increase. Therefore, a compromise between precision and cost dictates the number of images that are analyzed. The typical standard error was 20–30% of the mean for ambient samples. Triplicate or duplicate sample analysis further verified the measurement uncertainties.

Particle volume (V) and density (d) are required to estimate bioaerosol mass contributions. The first-order calculation assumes spherical particles (Tai et al., 2017), thus:

$$V = \frac{\pi}{6}(D_{eq,A})^3 \quad (2)$$

Depending on the bioaerosol type, particle density ranges from 0.9 to 1.5 g cm^{-3} (Burge, 1995; Cox and Wathes, 1995). A density of 1 g cm^{-3} (Matthias-Maser and Jaenicke, 2000; Chow et al., 2015) was assumed for this study. Outlier images were excluded from the calculation of total or size-segregated number/mass concentrations. Bioaerosol number and mass loading densities were calculated in cm^{-2} and g cm^{-2} , respectively, and converted to ambient concentrations, i.e., cm^{-3} (or 10^6 m^{-3}) and $\mu\text{g m}^{-3}$, using recorded MiniVol sample durations, flow rates, and filter deposit areas (Table S1).

3. Results and discussion

3.1. Bioaerosol number and size measurements

Bioaerosol counts from DS-FM reproduced the concentrations for standard samples across two orders of magnitude dynamic range with slopes close to unity (Fig. 2). The DS protocol appears to sufficiently mark the bioaerosols. Blank samples showed particle counts of $1\text{--}2 \times 10^3 \text{ cm}^{-2}$, resulting in a LQL of $6 \times 10^3 \text{ cm}^{-2}$ or $\sim 0.01 \text{ cm}^{-3}$ ambient concentration (i.e., 3 times standard deviations of the blank levels). For *E. coli*, the measurement precision (from replicate standard samples) was within $\pm 10\%$ for concentrations > 10 times the LQL. Precisions up to $\pm 20\%$ were found for the fungal spore standards. This larger uncertainty might be partly due to non-uniformity of the bioaerosol deposits, as the *A. fumigatus* spores were not as homogeneously dispersed in solution as were the *E. coli* cells. When the bacteria cells/fungal spores were deposited on preloaded $\text{PM}_{2.5}$ or PM_{10} samples, instead of blank BPC filters, the regression slopes were similar, consistent with minimal interferences in bioaerosol staining and counting (Kolberg, 2017).

Ambient bioaerosol concentrations by DS-FM (averaged over triplicates) ranged $1.7 \times 10^4 \text{--} 2.4 \times 10^5 \text{ cm}^{-2}$ for $\text{PM}_{2.5}$ and $3.4 \times 10^4 \text{--} 6.0 \times 10^5 \text{ cm}^{-2}$ for PM_{10} (Table 1), substantially above the LQL. ES-FM generally reported lower bioaerosol counts, on average only $\sim 50\%$ of those measured by DS-FM. This is consistent with insufficient extraction and/or particle loss during the wash-off and re-deposition steps. Excluding counts less than 10 times the LQL, triplicate precision for DS-FM was shown to be $\sim \pm 30\%$ (Fig. 3). Part of this is attributed to nonhomogeneous filter deposits, which can vary by up to 30% depending on the particle size and inlet type (Hyslop and White, 2008; Schichtel et al., 2008). On the other hand, replicate precision for ES-FM was $\sim \pm 75\%$ ($\text{PM}_{2.5}$) and $\sim \pm 55\%$ (PM_{10}) (Fig. 3). Owing to this large uncertainty, ES-FM results are not discussed further.

Fig. 4a compares typical number-size distribution of *E. coli* and *A. fumigatus* spores as determined by DS-FM. $D_{eq,A}$ of *E. coli* were mostly ($\sim 70\%$) found between 1 and $2.2 \mu\text{m}$, consistent with the dimensions measured by atomic force microscopy (Amro et al., 2000; Osiro et al., 2012). Smaller particle sizes ($< 1 \mu\text{m}$) likely resulted from cell fragmentation or irregular orientation of *E. coli* cells on the filter, thereby producing smaller projected areas. *A. fumigatus* spores showed a broader size distribution with 70% of $D_{eq,A}$ ranging from 0.75 to $2.2 \mu\text{m}$. Similarly, Deacon et al. (2009) reported the highest concentrations of *A. fumigatus* spores (single cell) in the range of 1– $2 \mu\text{m}$ diameter, as well as many smaller particles between 0.65 and $1 \mu\text{m}$. A minor fraction ($< 0.5\%$) of large particles ($> 4 \mu\text{m}$) found among both *E. coli* cells and *A. fumigatus* spores in this study might be attributed to cell clumps or aggregates.

In contrast, size distributions for the ambient samples in Fig. 4b extended more into the smaller and larger size ranges, reflecting the diverse nature of real-world biological particles. Coarse particles ($D_{eq,A} > 2.5 \mu\text{m}$) accounted for 14% and 21% of bioaerosol counts in $\text{PM}_{2.5}$ and PM_{10} , respectively, throughout our sampling period. $\text{PM}_{2.5}$ samples contained particles $> 2.5 \mu\text{m}$ because the MiniVol inlet is based on the aerodynamic instead of geometric diameter and the sampling effectiveness curve passes some coarse particles with $< 50\%$ penetration efficiency (Hill et al., 1999; Buser et al., 2007).

The tests with standard bioaerosols show the feasibility of resolving bioaerosol size mode with DS-FM. Compared with results from real-time fluorescence sensors such as UV-APS and WIBS (Huffman et al., 2010, 2012; Healy et al., 2014), DS-FM appears to report more abundant submicron particles. While some bacteria, fungal fragments, and viruses fall in this size range, the measurement of smaller bioaerosols, especially those $< 0.7 \mu\text{m}$, present bigger challenges for both the real-time and microscopic methods. These particles, however, are not expected to contribute significantly to bioaerosol mass in most situations.

3.2. Bioaerosol contributions to fine and coarse PM

Table 1 presents the range of ambient bioaerosol number concentrations, which are generally on the order of $0.1\text{--}1 \text{ cm}^{-3}$ with $\sim 50\%$ higher values found in PM_{10} than in $\text{PM}_{2.5}$ samples. Concurrent microscopic spore counts ranged from 1.5×10^{-4} to $2.3 \times 10^{-3} \text{ cm}^{-3}$

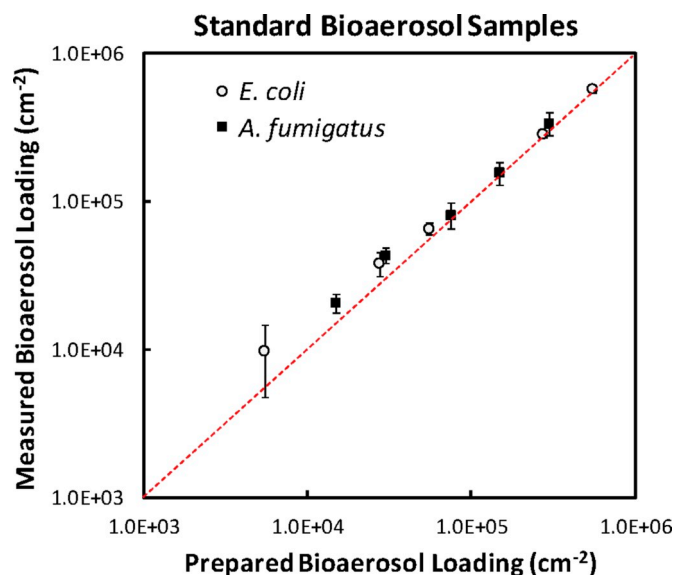


Fig. 2. DS-FM quantified versus laboratory prepared bioaerosol loadings on standard samples. Values and error bars are based on the average and standard deviation over four replicate experiments. The red dashed line indicates the 1:1 correspondence. (For interpretation of the references to color in this figure legend, the reader is referred to the Web version of this article.)

Table 1
Bioaerosol number concentrations (in cm^{-2}) for ambient $\text{PM}_{2.5}$ and PM_{10} samples quantified by DS-FM and ES-FM methods.

	DS-FM		ES-FM	
	$\text{PM}_{2.5}$	PM_{10}	$\text{PM}_{2.5}$	PM_{10}
# of Valid Samples ^a	59	56	55	55
Average	7.0×10^4 (0.17) ^b	1.1×10^5 (0.27)	3.9×10^4 (0.09)	5.4×10^4 (0.13)
Median	5.6×10^4 (0.14)	8.8×10^4 (0.21)	3.2×10^4 (0.08)	4.6×10^4 (0.11)
Minimum	1.7×10^4 (0.04)	3.4×10^4 (0.08)	1.4×10^4 (0.03)	1.4×10^4 (0.03)
Maximum	2.4×10^5 (0.57)	6.0×10^5 (1.45)	1.3×10^5 (0.30)	2.1×10^5 (0.47)

^a 24-hr samples collected by MiniVol sampler in Las Vegas, Nevada (4/1/2017–5/31/2017).

^b Values in the parentheses are the corresponding ambient number concentrations in cm^{-3} .

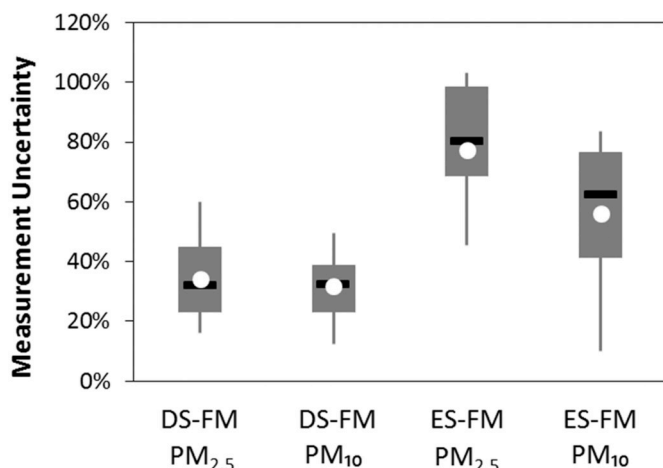


Fig. 3. Statistical distribution of DS-FM and ES-FM measurement precision (% uncertainty) for bioaerosol counts on individual PM samples, based on triplicate (DS-FM) or duplicate (ES-FM) analysis. Only loadings higher than 10 times the LQL of $6 \times 10^3 \text{ cm}^{-2}$ are taken into account. Circle indicates mean, black horizontal line indicates median, box bottom and top indicate 25th and 75th percentiles, and upper and lower whiskers indicate 10th and 90th percentiles.

with an average of $8.0 \times 10^{-4} \text{ cm}^{-3}$. Pollen counts ranged from 7.8×10^{-6} to $5.4 \times 10^{-4} \text{ cm}^{-3}$ with an average of $1.1 \times 10^{-4} \text{ cm}^{-3}$. These fungal spore and pollen counts are at the low end of nominal ambient levels (i.e., $10^{-2} - 10^{-3} \text{ cm}^{-3}$ for fungal spores and $10^{-5} - 10^{-3} \text{ cm}^{-3}$ for pollen; see Després et al., 2012) and explain < 1% of the bioaerosols. Many fungal species have not been included in the NAB Pollen and Mold Report; hyphal fragments, mostly submicron particles and uncounted, can be in much higher concentrations than spores (Green et al., 2006). In addition, many pollen grains were excluded by the MiniVol inlet due to their larger sizes. It is likely that airborne bacteria, unidentified fungal spores and fragments, as well as their derivatives contributed substantially to the observed bioaerosols.

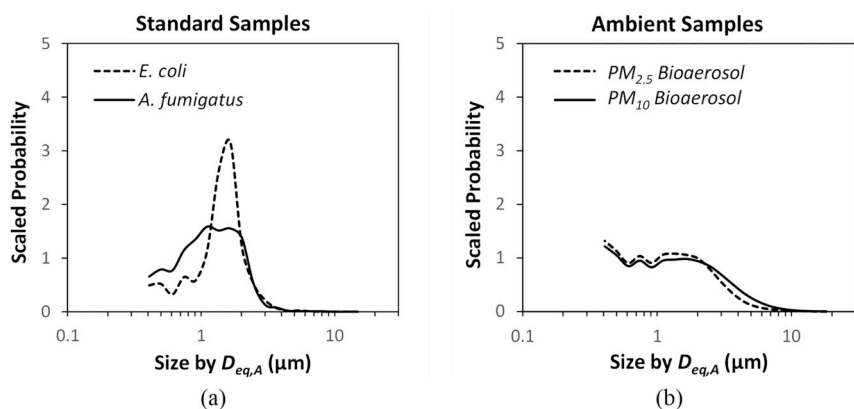


Fig. 4. Number-size distributions of: (a) standard and (b) ambient bioaerosol samples measured by DS-FM. Particles were counted by equally spaced 20 size bins in logarithmic space between 0.37 and 16 μm and averaged over all standard or ambient samples (see Table 1 for the number of ambient samples). Scaled probabilities indicate probability density in the log-space.

Wide bioaerosol concentration ranges have been reported (Table 2), depending on sampling location, season, bioaerosol type, and analytical method. The Las Vegas results fall within and at the lower end of values derived from DS-FM or ES-FM measurements in urban areas, despite the potential particle loss with ES-FM methods. This more or less reflects the arid climate of Las Vegas which is not conducive to dense vegetation. Nevertheless, ~25% of Las Vegas's two-million residents suffer from seasonal allergies (Tavares, 2010). Real-time autofluorescence methods including UV-APS and WIBS are known to report lower bioaerosol counts, as not all bioaerosols fluoresce under their excitation conditions and the detection efficiency decreases substantially for particle diameters < 0.7 μm (Huffman et al., 2010; Després et al., 2012). Based on UV-APS, Wei et al. (2016) and Huffman et al. (2012) showed peak bioaerosol sizes to be ~1–3 μm for both urban and remote areas. A similar peak is found in Las Vegas, with a secondary peak in the submicrometer range (Fig. 4). Prussin et al. (2015) reported virus-like bioaerosols with sizes < 0.5 μm and outdoor concentrations comparable to bioaerosols > 0.5 μm .

The reconstructed bioaerosol mass from Eq. (2) and assumed unit density exhibits a dominant contribution from coarse particles (Fig. 5). On average, $\text{PM}_{2.5}$ and PM_{10} bioaerosol mass concentrations were $1.2 \mu\text{g m}^{-3}$ and $3.3 \mu\text{g m}^{-3}$, respectively. Day-to-day bioaerosol mass concentrations varied by a factor of 8 ($0.45\text{--}3.5 \mu\text{g m}^{-3}$) for $\text{PM}_{2.5}$ and by a factor of 20 ($1.2\text{--}23.8 \mu\text{g m}^{-3}$) for PM_{10} . Concurrently, 24-h $\text{PM}_{2.5}$ mass concentrations (by CCDAQ) ranged from 4.0 to 10.8 $\mu\text{g m}^{-3}$ with an average of 6.8 $\mu\text{g m}^{-3}$ while PM_{10} ranged from 8.4 to 36.9 $\mu\text{g m}^{-3}$ with an average of 17.8 $\mu\text{g m}^{-3}$. On a daily basis, bioaerosols accounted for $18 \pm 8\%$ and $17 \pm 11\%$ of $\text{PM}_{2.5}$ and PM_{10} mass, respectively. This could be an overestimate for $\text{PM}_{2.5}$, since coarse bioaerosols found on the $\text{PM}_{2.5}$ samples substantially inflate the mass calculations. Moreover, the $\text{PM}_{2.5}$ size cut is based on aerodynamic diameter rather than the projected geometric diameter.

A recent review by Fröhlich-Nowoisky et al. (2016) suggests that bioaerosols typically account for ~30% of number and mass concentrations of coarse particles (> 1 μm) in urban and rural air and as high as 80% in pristine rainforest air. If coarse bioaerosol mass was

Table 2
Bioaerosol number concentrations reported in recent studies by location, season, bioaerosol type, and analytical method.

Location	Site Type, Season	Bioaerosol Type	Bioaerosols (cm ⁻³)	Analytical Method	Reference
Blacksburg, VA, USA	Suburban, Fall	Bioaerosol 0.5–5 μm	0.84 ± 0.44	DS-FM, with SYBRGold ^a	Prussin et al. (2015)
Las Vegas, NV, USA	Urban, Spring	Bioaerosol 0.37–10 ^b μm	0.27 (0.08–1.5)	DS-FM, with DAPI	This study
Xi'an, China	Urban, Annual	Total bioaerosol	0.40 (0.077–1.4)	ES-FM, with DAPI	Xie et al. (2018)
Qingdao, China	Urban, Annual	Total bioaerosol	0.72 (0.085–2.1)	ES-FM, with DAPI	Dong et al. (2016)
Taipei, Taiwan	Urban, Summer	Total bioaerosol	0.77 (0.36–2.0)	ES-FM ^c , with DAPI	Chi and Li (2007)
Mt. Werner, CO, USA	Remote, Spring	Total bioaerosol	3.9 (1.0–6.6)	ES-FM, with DAPI	Wiedinmyer et al. (2009)
Mt. Rax, Austria	Remote, Annual	Bacteria	0.012 (0.007–0.019)	ES-FM ^c , with DAPI	Bauer et al. (2002)
		Fungal spore	0.001 (0–0.003)		
Corcoran, CA, USA	Agriculture, Fall	Fungal spore	0.071 (0.035–0.11)	SEM	Chow et al. (2015)
		Pollen grain	0.003 (0.001–0.006)		
Beijing, China	Urban, Winter	Bioaerosol > 0.5 μm	0.15 (0.005–0.66)	UV-APS	Wei et al. (2016)
Amazon Basin, Brazil	Remote, Summer	Bioaerosol > 1 μm	0.093 (0.040–0.13)	UV-APS	Huffman et al. (2012)
Rocky Mountain, USA	Remote, Summer	Bioaerosol > 0.5 μm	0.04 (0.01–0.08)	UV-APS	Gosselin et al. (2016)
Atlanta, GA, USA	Urban, Spring	Total bioaerosol	0.084 (0.019–0.19)	Flow Cytometry	Marty (2016)
			0.016 (0.003–0.066)	WIBS-3	
Helsinki, Finland	Urban, Winter	Bioaerosol 0.5–5 μm	0.14 (0.01–1.1)	BioScout ^d	Saari et al. (2015)
	Urban, Summer		0.046 (0.01–0.9)		

^a SYBRGold: A proprietary unsymmetrical cyanine dye for DNA and RNA. It costs ~50 times of DAPI.

^b Particles were collected after a PM₁₀ size-cut inlet, though large particles up to ~16 μm were observed on the filter.

^c Particles were collected in a solution (liquid), rather than on filter, and extraction is not required.

^d BioScout: A commercial 405 nm diode laser-based on-line bioaerosol detector.

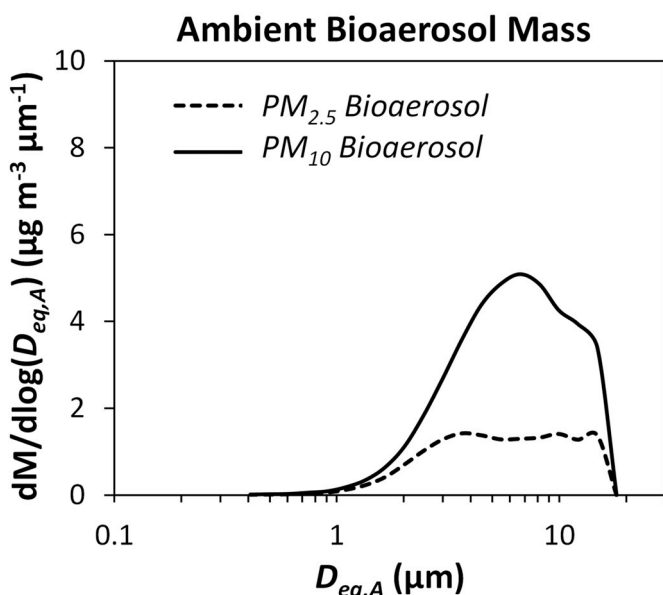


Fig. 5. DS-FM estimated mass-size distributions of ambient bioaerosol in PM_{2.5} and PM₁₀ samples. Bioaerosol mass (M) was calculated for equally spaced 20 size bins in logarithmic space between 0.37 and 16 μm and averaged over all ambient samples assuming spherical particles and unit density.

calculated from all detectable particles with 2.5–10 μm $D_{eq,A}$ in the PM₁₀ samples, it would account for $20 \pm 13\%$ of PM_{10-2.5} determined from the difference between PM₁₀ and PM_{2.5} mass in this study. On the other hand, fine bioaerosols (< 2.5 μm $D_{eq,A}$ found in PM₁₀ samples) would account for only $4 \pm 3\%$ of PM_{2.5} mass. Despite uncertainties in size, shape, and density assumptions for mass calculation, these consistent results show the potential of employing DS-FM to estimate size-segregated bioaerosol mass fractions in ambient PM.

3.3. Controlling factors for bioaerosol

Day-to-day variations of the bioaerosol number and mass concentrations, as well as daily PM_{2.5}/PM₁₀ levels and meteorology are presented in the supplementary information (Fig. S3). The highest bioaerosol concentrations (5/6–8/2017) occurred during and

immediately after the highest precipitation event throughout the study. On 5/7/2017, PM₁₀ bioaerosol mass ($23.8 \mu\text{g m}^{-3}$) was ~7 times the average ($3.3 \mu\text{g m}^{-3}$). Although the mechanisms are not entirely clear, precipitation has been associated with elevated bioaerosol concentrations elsewhere (Huffman et al., 2013; Kang et al., 2015; Rathnayake et al., 2017). Speciated fungi and pollen levels increased somewhat during the rain event, but the highest concentrations were recorded for other dry periods when the host plants matured.

Excluding the rainy periods, there is a moderate correlation of PM₁₀ bioaerosol mass (or number) concentrations with PM_{10-2.5} ($r = 0.62$ or 0.63 , $p \ll 0.01$). Correlations with PM_{2.5} are much less significant ($r = 0.22$ or 0.29 , $p = 0.12$ or 0.04). Wind speed is considered as a common factor influencing bioaerosol and PM_{10-2.5} concentrations. The monitoring days were classified into three wind conditions: 1) calm; 2) moderate; and 3) windy, according to the daily average and fastest 2-min wind speed, to examine the wind effect. As shown in Fig. 6a, windy conditions correspond to higher concentrations of bioaerosol, PM₁₀, and PM_{10-2.5} mass, followed by the moderate and calm wind conditions. The differences between the windy and calm conditions are statistically significant ($p < 0.01$). Wind, however, appears to have no effect on the PM_{2.5} mass concentration. With respect to bioaerosol number, Fig. 6b also shows a significant increase from the calm to the windy conditions. Fungi and pollen counts did not vary significantly for different wind conditions, though the highest pollen counts ($> 3 \times 10^{-4} \text{ cm}^{-3}$ or 300 m^{-3}) all occurred on windy days.

Strong winds can mechanically resuspend surface dust, thus re-aerosolizing PM_{10-2.5} as well as bioaerosols that previously settled on the surface and/or attached to dust particles. In addition, some spore and pollen species can only be released under wind speeds exceeding a certain threshold (Jones and Harrison, 2004). The resuspension mechanism better explains the observed bioaerosol-wind dependence here, considering the lack of clear correlation between bioaerosol and spore/pollen counts.

The opposite effects of wind and precipitation on bioaerosols have been reported in other regions (Li et al., 2017; Liu et al., 2019), possibly associated with enhanced dispersion and scavenging that lower the PM and bioaerosol levels simultaneously. Higher temporal resolution data from on-line sensors could further elucidate the correlation of winds and bioaerosol concentrations. A longer monitoring period with concurrent PM chemistry measurements will help study the bioaerosol sources using receptor modeling techniques.

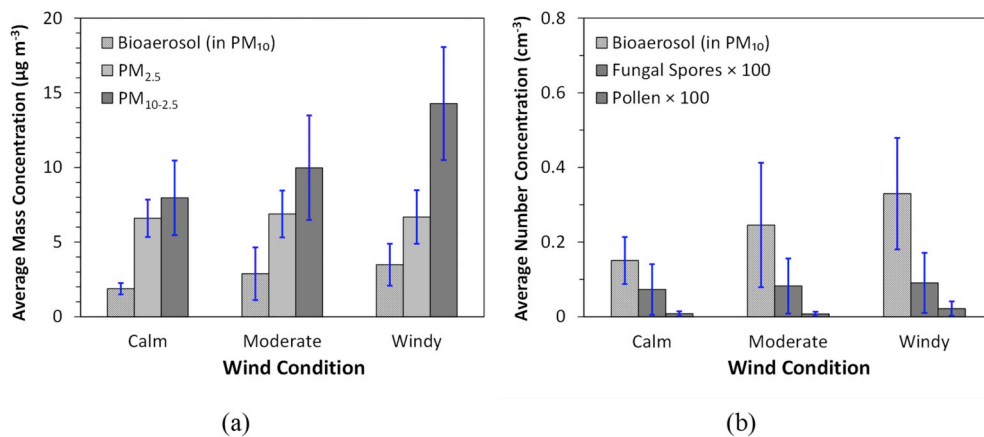


Fig. 6. PM and bioaerosol for: (a) mass and (b) number concentrations under calm (14 days), moderate (27 days), and windy (14 days) conditions. The “Calm” condition refers to a daily mean wind speed $\leq 2.6 \text{ m s}^{-1}$ and fastest 2-min wind speed $\leq 7.6 \text{ m s}^{-1}$ while the “Windy” condition referred to a daily mean wind speed $\geq 5.5 \text{ m s}^{-1}$ and fastest 2-min wind speed $\geq 10.3 \text{ m s}^{-1}$. The rest are considered as the “Moderate” condition. Fungi and pollen concentrations have been multiplied by 100. Error bars indicate the standard deviation.

4. Conclusion and recommendations

Bioaerosols are among the least quantified components in PM_{2.5} and PM₁₀. It was recognized by the U.S. EPA (2006), and is becoming more evident now, that bioaerosols including bacteria, fungi, pollen, etc. can be a major health risk of PM_{10-2.5}. However, it is challenging to establish the air quality standard or exposure limit around bioaerosols, partly due to the lack of standardized, extensively applicable methods for offline laboratory analyses or online, continuous monitoring (Walser et al., 2015). This study evaluated an epifluorescence method for its potential application to the routine air quality monitoring for quantifying bioaerosol concentration and size distribution as well as establishing their contribution to PM_{2.5} and PM₁₀. This method (i.e., DS-FM) involves collecting PM on BPC filters using common ambient air quality samplers, directly staining deposits on the filter with a DNA marker, imaging the sample using a fluorescence microscope, and counting/counting bioaerosols automatically from the images.

DS-FM is cost effective, with relatively short turnaround times, and allows for repeat analysis on the same sample. Compared with the more conventional ES-FM method, which stains particles in a liquid, DS-FM appears to better avoid contamination and/or particle loss throughout the analysis. Testing with standard bioaerosol samples made of bacterial cells and fungal spores showed good accuracy and precision of DS-FM counts for a dynamic range more than two orders of magnitude. This range (10^4 – 10^6 cm^{-2} on the filter or 0.01 – 1 cm^{-3} in the air if sampled by a MiniVol for 24 h) should allow bioaerosol monitoring in most outdoor environments. Reasonable size distributions were reported for the type of microbe according to the equivalent projected area diameter, with a lower size detection limit of $\sim 0.37 \mu\text{m}$. The DS-FM is recommended for off-line PM monitoring. Compared to on-line bioaerosol sensors, it offers less temporal resolution but potentially more spatial and longer-term coverages.

Results of ambient bioaerosol measurements by DS-FM for Las Vegas, Nevada during springtime compare reasonably with those measured elsewhere. The time resolution is limited to 24 h, but it is sufficient to support the important role of precipitation and wind in controlling outdoor bioaerosol levels. However, the measurement precision may be improved further by reducing nonhomogeneous particle deposition on a filter. Coarse bioaerosol particles were found in PM_{2.5} samples, partly due to the inefficient size-cutoff of MiniVol samplers, and this could substantially inflate the bioaerosol contribution to PM_{2.5} mass if it includes all bioaerosol particles detected in the PM_{2.5} samples. To minimize these issues, samplers with a sharp size-cut inlet, similar to the design of Federal Reference Method (Vanderpool et al., 2008), are recommended when applying DS-FM in parallel to compliance PM monitoring. Bioaerosols measured in PM_{2.5} samples should be reconciled with the fine fraction ($D_{eq,A} < 2.5 \mu\text{m}$) in PM₁₀ samples.

DS-FM provides a first-order estimate of size-segregated bioaerosol

mass, which may serve as a bioaerosol marker in receptor modeling for more detailed PM source apportionment, similar to the use of potassium as a wood smoke marker and silicon as a fugitive dust marker (Watson et al., 2008; Chen and Cao, 2018). This will further inform the bioaerosol contribution and origins. Moreover, by extensively evaluating associations of bioaerosols with PM_{2.5}, PM₁₀, and PM_{10-2.5} concentrations as well as health endpoints such as incidence of allergy, asthma, and other respiratory illnesses, it paves the way to a critical air quality standard and/or exposure limit to protect public health.

Acknowledgements

The authors acknowledge financial support from the School of Public Health, University of Nevada, Las Vegas and the Environmental Analysis Facility, Desert Research Institute. The participation of Ting Liu was supported by an exchange scholar grant from the Hubei Province of China (D20184502). Pollen and fungal spore monitoring was sponsored by the Clark County School District.

Appendix A. Supplementary data

Supplementary data to this article can be found online at <https://doi.org/10.1016/j.atmosenv.2019.05.051>.

Declaration of interests

The authors declare that they have no known competing financial interests or personal relationships that could have appeared to influence the work reported in this paper.

References

- Asthma and Allergy Foundation of America (AAFA), 2018. Allergy Capitals Spring 2018. pp. 8. Retrieved 4/24/2019 from: <http://www.aaafa.org/media/AAFA-2018-Spring-Allergy-Capitals-Report.pdf>.
- Amro, N.A., Kotra, L.P., Wadu-Mesthrige, K., Bulychev, A., Mobashery, S., Liu, G.Y., 2000. High-resolution atomic force microscopy studies of the Escherichia coli outer membrane: structural basis for permeability. *Langmuir* 16 (6), 2789–2796. <https://doi.org/10.1021/la991013x>.
- Bauer, H., Kasper-Giebl, A., Löflund, M., Giebl, H., Hitzberger, R., Zibuschka, F., Puxbaum, H., 2002. The contribution of bacteria and fungal spores to the organic carbon content of cloud water, precipitation and aerosols. *Atmos. Res.* 64 (1–4), 109–119. [https://doi.org/10.1016/S0169-8095\(02\)00084-4](https://doi.org/10.1016/S0169-8095(02)00084-4).
- Blais-Lecours, P., Perrott, P., Duchaine, C., 2015. Non-culturable bioaerosols in indoor settings: impact on health and molecular approaches for detection. *Atmos. Environ.* 110, 45–53. <https://doi.org/10.1016/j.atmosenv.2015.03.039>.
- Boreson, J., Dillner, A.M., Peccia, J., 2004. Correlating bioaerosol load with PM_{2.5} and PM₁₀ concentrations: a comparison between natural desert and urban-fringe aerosols. *Atmos. Environ.* 38 (35), 6029–6041. <https://doi.org/10.1016/j.atmosenv.2004.06.040>.
- Burge, H.A., 1995. *Bioaerosol Investigations*. Bioaerosols. Lewis Publishers, Boca Raton, FL 978-0873717243.
- Buser, M.D., Parnell, C.B., Shaw, B.W., Lacey, R.E., 2007. Particulate matter sampler

- errors due to the interaction of particle size and sampler performance characteristics: ambient PM_{2.5} samplers. *Transactions of the ASABE* 50 (1), 241–254. <https://doi.org/10.13031/2013.22405>.
- CCDAQ, 2014. Clark County Aeroallergen History and Cycles. Clark County Department of Air Quality, Las Vegas, NV. https://www.clarkcountynv.gov/airquality/monitoring/Pages/Monitoring_PollenReports.aspx.
- Chen, L.-W.A., Cao, J., 2018. PM_{2.5} source apportionment using a hybrid environmental receptor model. *Environ. Sci. Technol* 52 (11), 6357–6369. <https://doi.org/10.1021/acs.est.8b00131>.
- Chi, M.C., Li, C.S., 2007. Fluorochrome in monitoring atmospheric bioaerosols and correlations with meteorological factors and air pollutants. *Aerosol Sci. Technol.* 41 (7), 672–678. <https://doi.org/10.1080/02786820701383181>.
- Chow, J.C., 1995. Measurement methods to determine compliance with ambient air quality standards for suspended particles. *J. Air Waste Manag. Assoc.* 45 (5), 320–382. <https://doi.org/10.1080/10473289.1995.10467369>.
- Chow, J.C., Yang, X., Wang, X., Kohl, S.D., Hurbain, P.R., Chen, L.-W.A., Watson, J.G., 2015. Characterization of ambient PM₁₀ bioaerosols in a California agricultural town. *Aerosol Air Qual. Res* 15 (4), 1433–1447. <https://doi.org/10.4209/aaqr.2014.12.0313>.
- Cox, C.S., Wathes, C.M., 1995. *Bioaerosols Handbook*. Lewis Publishers, Boca Raton, FL 9780873716154.
- Deacon, L.J., Pankhurst, L.J., Drew, G.H., Hayes, E.T., Jackson, S., Longhurst, P.J., Longhurst, J.W.S., Liu, J., Pollard, S.J.T., Tyrrel, S.F., 2009. Particle size distribution of airborne *Aspergillus fumigatus* spores emitted from compost using membrane filtration. *Atmos. Environ.* 43 (35), 5698–5701. <https://doi.org/10.1016/j.atmosenv.2009.07.042>.
- Deguillaume, L., Leriche, M., Amato, P., Ariya, P.A., Delort, A.M., Pöschl, U., Chaumerliac, N., Bauer, H., Flossmann, A., Morris, C.E., 2008. Microbiology and atmospheric processes: chemical interactions of primary biological aerosols. *Biogeosciences* 5, 1073–1084.
- Després, V., Huffman, J.A., Burrows, S.M., Hoose, C., Safatov, A., Buryak, G., Fröhlich-Nowoisky, J., Elbert, W., Andreae, M., Pöschl, U., Jaenicke, R., 2012. Primary biological aerosol particles in the atmosphere: a review. *Tellus B: Chem. Phys. Meteorol.* 64 (1), 15598. <https://doi.org/10.3402/tellusb.v64i0.15598>.
- Dong, L., Qi, J., Shao, C., Zhong, X., Gao, D., Cao, W., Gao, J., Bai, R., Long, G., Chu, C., 2016. Concentration and size distribution of total airborne microbes in hazy and foggy weather. *Sci. Total Environ.* 541, 1011–1018. <https://doi.org/10.1016/j.scitotenv.2015.10.001>.
- Douwes, J., Thorne, P., Pearce, N., Heederik, D., 2003. Bioaerosol health effects and exposure assessment: progress and prospects. *Ann. Occup. Hyg.* 47 (3), 187–200. <https://doi.org/10.1093/annhyg/meg032>.
- Fröhlich-Nowoisky, J., Pickersgill, D.A., Després, V.R., Pöschl, U., 2009. High diversity of fungi in air particulate matter. *Proc. Natl. Acad. Sci. Unit. States Am.* 106 (31), 12814–12819. <https://doi.org/10.1016/j.atmosres.2016.07.018>.
- Fröhlich-Nowoisky, J., Kampf, C.J., Weber, B., Huffman, J.A., Pöhlker, C., Andreae, M.O., Lang-Yona, N., Burrows, S.M., Gunthe, S.S., Elbert, W., Su, H., 2016. Bioaerosols in the Earth system: climate, health, and ecosystem interactions. *Atmos. Res.* 182, 346–376. <https://doi.org/10.1073/pnas.0811003106>.
- Gosselin, M.I., Rathnayake, C.M., Crawford, L., Pöhlker, C., Fröhlich-Nowoisky, J., Schmer, B., Després, V.R., Engling, G., Gallagher, M., Stone, E., Pöschl, U., 2016. Fluorescent bioaerosol particle, molecular tracer, and fungal spore concentrations during dry and rainy periods in a semi-arid forest. *Atmos. Chem. Phys.* 16 (23), 15165–15184. <https://doi.org/10.5194/acp-16-15165-2016>.
- Green, B.J., Tovey, E.R., Sercombe, J.K., Blachere, F.M., Beezhold, D.H., Schmechel, D., 2006. Airborne fungal fragments and allergenicity. *Med. Mycol.* 44 (Suppl. ment_1), S245–S255. <https://doi.org/10.1080/13693780600776308>.
- Griffin, D.W., Garrison, V.H., Herman, J.R., Shinn, E.A., 2001. African desert dust in the Caribbean atmosphere: microbiology and public health. *Aerobiologia* 17 (3), 203–213. <https://doi.org/10.1023/A:101186821>.
- Hand, J.L., Schichtel, B.A., Pitchford, M., Malm, W.C., Frank, N.H., 2012. Seasonal composition of remote and urban fine particulate matter in the United States. *J. Geophys. Res.: Atmosphere* 117, D05209. <https://doi.org/10.1029/2011JD017122>.
- Healy, D.A., Huffman, J.A., O'Connor, D.J., Pöhlker, C., Pöschl, U., Sodeau, J.R., 2014. Ambient measurements of biological aerosol particles near Killarney, Ireland: a comparison between real-time fluorescence and microscopy techniques. *Atmos. Chem. Phys.* 14 (15), 8055–8069. <https://doi.org/10.5194/acp-14-8055-2014>.
- Hill, J.S., Patel, P.D., Turner, J.R., 1999. June. Performance characterization of the MiniVol PM_{2.5} sampler. In: *Air and Waste Management Association's 92nd Annual Meeting*. Paper, Pittsburgh, Pennsylvania, pp. 99–617.
- Huffman, J.A., Treutlein, B., Pöschl, U., 2010. Fluorescent biological aerosol particle concentrations and size distributions measured with an Ultraviolet Aerodynamic Particle Sizer (UV-APS) in Central Europe. *Atmos. Chem. Phys.* 10 (7), 3215–3233. <https://doi.org/10.5194/acp-10-3215-2010>.
- Huffman, J.A., Sinha, B., Garland, R.M., Snee-Pollmann, A., Gunthe, S.S., Artaxo, P., Martin, S.T., Andreae, M.O., Pöschl, U., 2012. Size distributions and temporal variations of biological aerosol particles in the Amazon rainforest characterized by microscopy and real-time UV-APS fluorescence techniques during AMAZE-08. *Atmos. Chem. Phys.* 12 (24), 11997–12019. <https://doi.org/10.5194/acp-12-11997-2012>.
- Huffman, J.A., Prenni, A.J., DeMott, P.J., Pöhlker, C., Mason, R.H., Robinson, N.H., Fröhlich-Nowoisky, J., Tobo, Y., Després, V.R., Garcia, E., Gochis, D.J., 2013. High concentrations of biological aerosol particles and ice nuclei during and after rain. *Atmos. Chem. Phys.* 13 (13), 6151. <https://doi.org/10.5194/acp-13-6151-2013>.
- Hyslop, N.P., White, W.H., 2008. An evaluation of interagency monitoring of protected visual environments (IMPROVE) collocated precision and uncertainty estimates. *Atmos. Environ.* 42 (11), 2691–2705. <https://doi.org/10.1016/j.atmosenv.2007.06.053>.
- Jones, A.M., Harrison, R.M., 2004. The effects of meteorological factors on atmospheric bioaerosol concentrations—a review. *Sci. Total Environ.* 326 (1–3), 151–180. <https://doi.org/10.1016/j.scitotenv.2003.11.021>.
- Kang, S.M., Heo, K.J., Lee, B.U., 2015. Why does rain increase the concentrations of environmental bioaerosols during monsoon. *Aerosol Air Qual. Res* 15, 2320–2324. <https://doi.org/10.4209/aaqr.2014.12.0328>.
- Kepner, R.L., Pratt, J.R., 1994. Use of fluorochromes for direct enumeration of total bacteria in environmental samples: past and present. *Microbiol. Rev.* 58 (4), 603–615.
- Kolberg, R., 2017. Evaluation of a Fluorescence Method for Quantifying Bioaerosol Concentrations on Air Quality Filter Samples (Master Thesis). Retrieved from University of Nevada, Las Vegas Library.
- Li, C.S., Huang, T.Y., 2006. Fluorochrome in monitoring indoor bioaerosols. *Aerosol Sci. Technol.* 40 (4), 237–241. <https://doi.org/10.1080/02786820500543308>.
- Li, Y., Lu, R., Li, W., Xie, Z., Song, Y., 2017. Concentrations and size distributions of viable bioaerosols under various weather conditions in a typical semi-arid city of Northwest China. *J. Aerosol Sci.* 106, 83–92. <https://doi.org/10.1016/j.jaerosci.2017.01.007>.
- Liu, T., Chen, L.-W.A., Zhang, M., Watson, J.G., Chow, J.C., Cao, J., Chen, H., Wang, W., Zhang, J., Zhan, C., Liu, H., 2019. Bioaerosol concentrations and size distributions during the autumn and winter seasons in an industrial city of Central China. *Aerosol and Air Quality Research* 19, 1095–1104. <https://doi.org/10.4209/aaqr.2018.11.0422>. (in press).
- Matthias-Maser, S., Bogs, B., Jaenicke, R., 2000. The size distribution of primary biological aerosol particles in cloud water on the mountain Kleiner Feldberg/Taunus (FRG). *Atmos. Res.* 54 (1), 1–13. [https://doi.org/10.1016/S0169-8095\(00\)00039-9](https://doi.org/10.1016/S0169-8095(00)00039-9).
- Marty, A.N., 2016. Understanding the Link between Meteorology and Speciated Abundance of Bioaerosols in an Urban Environment (Master Thesis). Retrieved from Georgia Tech Library.
- Mauderly, J.L., Chow, J.C., 2008. Health effects of organic aerosols. *Inhal. Toxicol.* 20 (3), 257–288. <https://doi.org/10.1080/08958370701866008>.
- Nasir, Z.A., Hayes, E., Williams, B., Gladding, T., Rolph, C., Khera, S., Jackson, S., Bennett, A., Collins, S., Parks, S., Attwood, A., 2019. Scoping studies to establish the capability and utility of a real-time bioaerosol sensor to characterise emissions from environmental sources. *Sci. Total Environ.* 648, 25–32. <https://doi.org/10.1016/j.scitotenv.2018.08.120>.
- Navidi, W.C., 2008. *Statistics for Engineers and Scientists*. McGraw-Hill Higher Education, New York, NY 978-0073376332.
- Osiro, D., Bernardes Filho, R., Assis, O.B.G., Jorge, L.A.D.C., Colnago, L.A., 2012. Measuring bacterial cells size with AFM. *Braz. J. Microbiol.* 43 (1), 341–347. <https://doi.org/10.1590/S1517-83822012000100040>.
- Patel, T.Y., Buttner, M., Rivas, D., Cross, C., Bazylinski, D.A., Seggev, J., 2018a. Variation in airborne pollen concentrations among five monitoring locations in a desert urban environment. *Environ. Monit. Assess.* 190 (7), 424. <https://doi.org/10.1007/s10661-018-6738-8>.
- Patel, T.Y., Buttner, M., Rivas, D., Cross, C., Bazylinski, D.A., Seggev, J., 2018b. Variation in airborne fungal spore concentrations among five monitoring locations in a desert urban environment. *Environ. Monit. Assess.* 190 (11), 634. <https://doi.org/10.1007/s10661-018-7008-5>.
- Portnoy, J., Barnes, C., Barnes, C.S., 2004. The National Allergy Bureau: pollen and spore reporting today. *J. Allergy Clin. Immunol.* 114 (5), 1235–1238. <https://doi.org/10.1016/j.jaci.2004.07.062>.
- Peccia, J., Hernandez, M., 2006. Incorporating polymerase chain reaction-based identification, population characterization, and quantification of microorganisms into aerosol science: a review. *Atmos. Environ.* 40 (21), 3941–3961. <https://doi.org/10.1016/j.atmosenv.2006.02.029>.
- Perrino, C., Marcovecchio, F., 2016. A new method for assessing the contribution of primary biological atmospheric particles to the mass concentration of the atmospheric aerosol. *Environ. Int.* 87, 108–115. <https://doi.org/10.1016/j.envint.2015.11.015>.
- Prussin, A.J., Garcia, E.B., Marr, L.C., 2015. Total concentrations of virus and bacteria in indoor and outdoor air. *Environ. Sci. Technol. Lett.* 2 (4), 84–88. <https://doi.org/10.1021/acs.estlett.5b00050>.
- Rathnayake, C.M., Metwali, N., Jayarathne, T., Kettler, J., Huang, Y., Thorne, P.S., O'Shaughnessy, P.T., Stone, E.A., 2017. Influence of rain on the abundance of bioaerosols in fine and coarse particles. *Atmos. Chem. Phys.* 17 (3), 2459–2475. <https://doi.org/10.5194/acp-17-2459-2017>.
- Saari, S., Niemi, J., Rönkkö, T., Kuuluvainen, H., Järvinen, A., Pirjola, L., Aurela, M., Hillamo, R., Keskinen, J., 2015. Seasonal and diurnal variations of fluorescent bioaerosol concentration and size distribution in the urban environment. *Aerosol Air Qual. Res* 15, 572–581. <https://doi.org/10.4209/aaqr.2014.10.0258>.
- Schichtel, B.A., Malm, W.C., Bench, G., Fallon, S., McDade, C.E., Chow, J.C., Watson, J.G., 2008. Fossil and contemporary fine particulate carbon fractions at 12 rural and urban sites in the United States. *J. Geophys. Res.: Atmosphere* 113, D02311. <https://doi.org/10.1029/2007JD008605>.
- Seo, I., Jha, B.K., Lim, J.G., Suh, S.I., Suh, M.H., Baek, W.K., 2014. Identification of lysosomal compounds based on the distribution and size of lysosomes. *Biochem. Biophys. Res. Commun.* 450 (1), 189–194. <https://doi.org/10.1016/j.bbrc.2014.05.091>.
- Tai, A.Y.-C., Chen, L.-W.A., Wang, X., Chow, J.C., Watson, J.G., 2017. Atmospheric deposition of particles at a sensitive alpine lake: size-segregated daily and annual fluxes from passive sampling techniques. *Sci. Total Environ.* 579, 1736–1744. <https://doi.org/10.1016/j.scitotenv.2016.11.117>.
- Tavares, S., 2010. Climate Change Creating Boom of Allergy-Causing Plants. Report Number May 13. Retrieved 4/24/2019 from: <http://www.lasvegassun.com/news/2010/may/13/attack-allergies/>.
- U.S. EPA, 2006. National ambient air quality standards for particulate matter: proposed

- rule. *Fed. Regist.* 71 (10), 2620–2708.
- Vanderpool, R., Kaushik, S., Houyoux, M., 2008. Laboratory Determination of Particle Deposition Uniformity on Filters Collected Using Federal Reference Method Samplers. U.S. EPA Report: EPA-HQ-OAR-2006-0735 (October 7, 2008). Retrieved 4/24/2019 from: <https://www3.epa.gov/ttn/naaqs/standards/pb/data/20081007LabDetermination.pdf>.
- Wagner, J., Macher, J., 2012. Automated spore measurements using microscopy, image analysis, and peak recognition of near-monodisperse aerosols. *Aerosol Sci. Technol.* 46 (8), 862–873. <https://doi.org/10.1080/02786826.2012.674232>.
- Walser, S.M., Gerstner, D.G., Brenner, B., Bünger, J., Eikmann, T., Janssen, B., Kolb, S., Kolk, A., Nowak, D., Raulf, M., Sagunski, H., 2015. Evaluation of exposure–response relationships for health effects of microbial bioaerosols—a systematic review. *Int. J. Hyg Environ. Health* 218 (7), 577–589. <https://doi.org/10.1016/j.ijheh.2015.07.004>.
- Watson, J.G., Chen, L.-W.A., Chow, J.C., Doraiswamy, P., Lowenthal, D.H., 2008. Source apportionment: findings from the US supersites program. *J. Air Waste Manag. Assoc.* 58 (2), 265–288. <https://doi.org/10.3155/1047-3289.58.2.265>.
- Wei, K., Zou, Z., Zheng, Y., Li, J., Shen, F., Wu, C.Y., Wu, Y., Hu, M., Yao, M., 2016. Ambient bioaerosol particle dynamics observed during haze and sunny days in Beijing. *Sci. Total Environ.* 550, 751–759. <https://doi.org/10.1016/j.scitotenv.2016.01.137>.
- Wiedinmyer, C., Bowers, R.M., Fierer, N., Horanyi, E., Hannigan, M., Hallar, A.G., McCubbin, I., Baustian, K., 2009. The contribution of biological particles to observed particulate organic carbon at a remote high altitude site. *Atmos. Environ.* 43 (28), 4278–4282. <https://doi.org/10.1016/j.atmosenv.2009.06.012>.
- Xie, Z., Li, Y., Lu, R., Li, W., Fan, C., Liu, P., Wang, J., Wang, W., 2018. Characteristics of total airborne microbes at various air quality levels. *J. Aerosol Sci.* 116, 57–65. <https://doi.org/10.1016/j.jaerosci.2017.11.001>.
- Zack, G.W., Rogers, W.E., Latt, S.A., 1977. Automatic measurement of sister chromatid exchange frequency. *J. Histochem. Cytochem.* 25 (7), 741–753. <https://doi.org/10.1177/25.7.70454>.
- Zhang, Z., Engling, G., Zhang, L., Kawamura, K., Yang, Y., Tao, J., Zhang, R., Chan, C.Y., Li, Y., 2015. Significant influence of fungi on coarse carbonaceous and potassium aerosols in a tropical rainforest. *Environ. Res. Lett.* 10 (3), 034015. <https://doi.org/10.1088/1748-9326/10/3/034015>.